Stimulation of Native Microorganisms for Biocementation in Samples Recovered from Field-Scale Treatment Depths

Michael G. Gomez, A.M.ASCE[1]; Charles M. R. Graddy[2]; Jason T. DeJong, M.ASCE[3]; Douglas C. Nelson[4]; and Michael Tsesarsky[5]

Abstract: Microbially induced calcite precipitation (MICP) is a biomediated cementation process that uses natural microbial enzymatic activity to improve the geotechnical properties of granular soils. In this study, two sets of experiments are completed using soil samples obtained from different depths to evaluate the feasibility of stimulating native ureolytic microorganisms for MICP at depths relevant to geotechnical applications. Batch and column experiments completed using five different stimulation solutions demonstrate that stimulation of native microbial ureolysis is improved with an enhanced stimulation solution, which differs from a standard stimulation solution used in previous studies through initial solution pH adjustment to 9.0 and higher concentrations of ammonium chloride and yeast extract of 100 mM and 0.2 g/L, respectively. A sterile sampling and column testing program is completed using soil materials obtained at shallow (2 m), middle (5.9 m), and deep (12 m) depths from a geotechnical boring and treated with both standard and enhanced stimulation solutions. Despite significant differences in stimulated urea degradation between soil depths and stimulation solution types, all tested columns achieved ureolysis rates sufficient to induce MICP, although at different times. Following 14 cementation treatments, soil columns achieved final V_s values as high as 1,020 m/s and unconfined compressive strengths as high as 1.9 MPa. The results of this study suggest that native ureolytic microorganisms may be successfully stimulated in natural soil deposits to induce calcite precipitation at treatment depths up to 12 m for geotechnical ground improvement. **DOI: 10.1061/(ASCE)GT.1943-5606.0001804.**

Introduction

Microbially induced calcite precipitation (MICP) is a promising biomediated cementation process which can improve the geotechnical properties of granular soils through the precipitation of calcium carbonate (calcite) on soil particle surfaces and at particle contacts (Stocks-Fisher et al. 1999; Martinez and DeJong 2009). The calcite precipitation reaction is made possible by microorganisms containing active urease enzymes, which, in the presence of urea, catalyze a hydrolysis reaction that generates ammonia and carbonic acid (Mobley et al. 1995)

$$CO(NH_2)_2 + 2H_2O \rightarrow 2NH_3 + H_2CO_3 \quad (1)$$

When the surrounding solution pH is not highly alkaline, produced ammonia will participate in an equilibrium reaction with water, resulting in some fraction protonating to become ammonium ions with an equal production of hydroxide ions. This hydroxide production promotes the deprotonation of carbonic acid to form increased concentrations of carbonate ions, which, in the presence of sufficient soluble calcium, may supersaturate aqueous solutions with respect to calcite and initiate calcite precipitation. Following biocementation, treated soils may exhibit increased initial shear stiffness, peak shear strength, and liquefaction resistance, with reductions in hydraulic conductivity and porosity (e.g., DeJong et al. 2006; Whiffin et al. 2007; Montoya et al. 2013; Gomez et al. 2014; Montoya and DeJong 2015).

Although successful demonstration of MICP soil improvement has been completed at a variety of scales (e.g., DeJong et al. 2006; Whiffin et al. 2007; Martinez and DeJong 2009; Bang et al. 2011; van Paassen 2011; Martinez et al. 2013; Gomez et al. 2015; DeJong et al. 2013), reliance on bioaugmentation, the injection of specialized nonnative bacterial strains (e.g., *Sporosarcina pasteurii*) to complete the process, has restricted the technology from becoming a cost-competitive alternative to other, more traditional ground improvement methods. Biostimulation, the use of selective substrates and/or environmental factors to stimulate the growth of native microorganisms with desirable metabolic capabilities, has been researched extensively in the field of bioremediation (e.g., Atlas and Bartha 1973; Gibson and Sewell 1992) with success in several notable field-scale applications (e.g., Pritchard and Costa 1991; Pritchard et al. 1992; Truex et al. 2009). Despite the frequent use of biostimulation in the field of bioremediation, few researchers have considered the use of this treatment technique for enabling MICP (Fujita et al. 2000, 2008; Burbank et al. 2011, 2013; Tobler et al. 2011; Gat et al. 2014, 2016; Gomez et al. 2014, 2016). Although some stimulated native species may complete ureolysis at rates slower than specialized laboratory cultivated bacterial strains (Hammes et al. 2003; Gomez et al. 2016), indigenous microorganisms may also be more resilient than augmented strains in natural subsurface environments (Armon and Arbel 1998; Acea et al. 1988),

[1]Assistant Professor, Dept. of Civil and Environmental Engineering, Univ. of Washington, Seattle, WA 98195. E-mail: mggomez@uw.edu

[2]Ph.D. Student, Dept. of Microbiology and Molecular Genetics, Univ. of California, Davis, CA 95616. E-mail: cmgraddy@ucdavis.edu

[3]Professor, Dept. of Civil and Environmental Engineering, Univ. of California, Davis, CA 95616 (corresponding author). E-mail: jdejong@ucdavis.edu

[4]Professor, Dept. of Microbiology and Molecular Genetics, Univ. of California, Davis, CA 95616. E-mail: dcnelson@ucdavis.edu

[5]Senior Lecturer, Dept. of Structural Engineering, Ben-Gurion Univ. of the Negev, Be'er Sheva 841050, Israel. E-mail: michatse@bgu.ac.il

Note. This manuscript was submitted on July 28, 2016; approved on June 15, 2017; published online on October 24, 2017. Discussion period open until March 24, 2018; separate discussions must be submitted for individual papers. This paper is part of the ***Journal of Geotechnical and Geoenvironmental Engineering***, © ASCE, ISSN 1090-0241.

enabling the possibility of more sustained ureolytic activity throughout the treatment process. Increases in spatial uniformity of improvement may also be achieved by eliminating limitations associated with cell transport through porous media. Perhaps most importantly, however, biostimulation for MICP may afford significant reductions in treatment implementation costs and detrimental environmental impacts related to energy and material usage by eliminating transportation and cultivation of bacterial inoculation solutions and potential ecological impacts related to the introduction of nonnative bacterial species (Litchman 2010).

Recent soil column experiments demonstrated successful stimulation of native ureolytic bacteria in quarried sands from various depositional environments with significant improvements in geotechnical properties after twenty cementation treatments (Gomez et al. 2014). More recently, a large-scale biocementation experiment demonstrated successful stimulation of native ureolytic microorganisms with transport distances at the meter-scale and nearly identical geotechnical improvement when compared with a second specimen treated using an augmentation approach (Gomez et al. 2016). Although these results are promising, the aforementioned experiments involved sands that were commercially processed at the ground surface and contained mixtures of materials from different depths, including surficial soils. Many geotechnical ground improvement applications, such as liquefaction mitigation, however, may require much deeper intervention to depths near 15 m. Concentrations of soil microorganisms are expected to decrease with depth due to reductions in soil organic matter, nutrient availability, and oxygen limitations (e.g., Fierer et al. 2003; Eilers et al. 2012), and the fraction of these deeper microorganisms that can complete urea hydrolysis sufficient to induce MICP as a function of soil depth is unknown. In order for stimulated MICP to become a viable alternative for geotechnical subsurface soil improvement, the effect of depth on ureolytic stimulation efficacy must be better understood.

In this study, two sets of experiments were completed using soil samples obtained at different depths from an aggregate quarry to evaluate the feasibility of stimulating native ureolytic microorganisms to induce MICP at depths relevant to ground improvement applications. First, solution optimization batch and column experiments were completed using soil samples obtained at different depths from a recently exposed cut slope to assess the performance of a standard stimulation solution used in previous experiments (Gomez et al. 2016) and the effect of novel stimulation techniques, including yeast extract and ammonium chloride additions, and solution pH adjustment. An enhanced stimulation solution was identified that improved stimulation of ureolysis by native soil microorganisms in samples obtained at depths near 10 m. A second experiment investigated ureolytic stimulation as a function of soil depth and compared the performance of the standard and enhanced stimulation solutions using soil samples obtained from a geotechnical boring. Samples were obtained at three depth intervals using sterile sampling procedures and prepared in two identical soil columns for each depth interval. Treatment solutions were applied to columns in a stimulation phase, during which either a standard or an enhanced stimulation solution was applied to stimulate native microorganisms, and in a cementation phase, during which soluble calcium was introduced to initiate calcite precipitation for a total of 14 treatments. Two additional columns, containing sterile glass beads, received similar treatments to control for biological contamination. During treatment, biogeochemical changes were monitored using total direct bacterial cell counts, aqueous urea, and solution pH measurements, and geotechnical improvement was monitored using shear-wave velocity (V_s) measurements. Post-treatment soil improvement was assessed using calcite content, unconfined compressive strength (UCS), final V_s, and scanning electron microscope (SEM) imaging of cemented soil specimens.

Materials and Methods

Site Soil Conditions

Soil samples were obtained at an aggregate quarry five miles west of Woodland, California near Cache Creek, a small local stream. The general subsurface stratigraphy at the site consisted of stiff clay to a depth of approximately 1.5 m; loose alluvial deposits of relatively clean sands, gravels, and interbedded clay lenses to depths ranging from 9 to 17 m; and stiff clay that persisted to depths beyond 30 m. At the boring location, stiff clay overburden material was encountered to a depth of 1.5 m, followed by deposits of clean and silty sand and gravel materials to a boring termination depth of 13.7 m. The groundwater table was measured at a similar depth of 13.7 m at a nearby monitoring well. Soil samples for solution optimization batch and column experiments were obtained at a cut slope approximately 300 m southwest of the boring location. Materials along this cut slope consisted of similar clean sand and gravel alluvial materials. Figs. 1(a and c) show the cut slope and boring locations, respectively.

Solution Optimization Experiments

Solution optimization batch and column experiments were completed to assess stimulation feasibility with depth and investigate the effect of ammonium chloride (NH_4Cl) and yeast extract (YE) additions and alkaline solution pH adjustment on native ureolytic stimulation. Soil samples for these experiments were obtained using autoclaved 1.2-m-long, 10.2-cm inner diameter (ID) aluminum sampling tubes driven horizontally into cut slopes [Fig. 1(b)]. All soil samples were collected no more than 4 h prior to the start of each test and were obtained approximately 1 m from the exposed slope surface at shallow (approximately 1 m), middle (approximately 5 m), or deep (approximately 10 m) depths below the original ground surface. Samples were sieved using sterile #4 sieves (4.76-mm openings) and homogenized in sterile rotating cylinders prior to testing. Batch experiments were completed in 500-mL sterile Erlenmeyer flasks containing 50 g of soil and a single 250-mL treatment solution volume, shaken continuously at 150 rpm. Column experiments were completed in autoclaved polycarbonate cylinders (10.2 cm high and 5.1 cm diameter) with daily treatment injections of 1.5 pore volumes (PV) using a sterile treatment system. All experiments were completed at a constant temperature of 20°C. Table 1 presents the composition of the modified A, modified B, modified C, standard, and enhanced stimulation solutions used in the solution optimization experiments. All stimulation solution variations contained identical concentrations of sodium acetate (42.5 mM) and urea (350 mM).

Sterile Field Sampling

Soil sampling was completed using hollow-stem auger drilling with driven California modified soil samplers (63.5-mm ID and 610-mm length) with drive shoes, nylon sand catchers, and internal 457-mm-long stainless-steel liners. Prior to sampling, samplers were preassembled, covered with aluminum foil on the exposed ends, and sterilized by autoclaving at 121°C for 60 min. Fig. 1(d) shows a sterile sampler being attached to an automatic trip hammer while the foil cover is being removed immediately prior to sampling. Sampling was completed at a single boring location at three discrete sampling intervals: shallow (1.5–2.4 m), middle

Fig. 1. (a) The cut slope location; (b) soil tube sampling; (c) geotechnical boring location; (d) sterile sampler immediately prior to sampling [(a–d) images by Michael G. Gomez]

Table 1. Treatment Solution Constituents and Concentrations

	Solution type					
Constituent	Modified A stimulation[a]	Modified B stimulation[a]	Modified C stimulation[a]	Standard stimulation[b]	Enhanced stimulation[b]	Cementation[b]
Yeast extract (g/L)	1.0	0.2	0.2	0.1	0.2	0.1
Ammonium chloride (mM)	12.5	12.5	200	12.5	100	12.5
Sodium acetate (mM)	42.5	42.5	42.5	42.5	42.5	42.5
Urea (mM)	350	350	350	350	350	350
Calcium chloride (mM)	—	—	—	—	—	250
Initial solution pH	7.3[c]	9.0[c]	9.0[c]	≈7.3	9.0[c]	≈8.4

[a]Treatment solution used only in solution optimization experiments.
[b]Treatment solution used in both solution optimization and boring column experiments.
[c]Denotes pH adjustment completed with NaOH.

(5.3–6.6 m), and deep (10.7–13.4 m); however, this study uses average sample depths of 2.0, 5.9, and 12.0 m, respectively, to refer to sample depths. In order to obtain material masses sufficient to prepare two soil columns, a minimum of two samples per discrete sampling interval were required; therefore, sterile samplers were driven in succession with sampling drives of 46 cm followed by 76 cm of soil auguring (30 cm through virgin material) and a subsequent sampling drive. During sampling, the center drill rod and pilot bit were removed from the center of the auger, brushed to remove soil debris, submerged in 70% ethanol solution, and flame sterilized before reuse. Following retrieval, samplers were opened and liners containing sampled soil materials were removed, plugged with #12 sterile rubber stoppers, and placed in a cooler at approximately 7°C for the remainder of sampling operations and transportation to the laboratory. Samplers and liners were not reused in order to mitigate biological cross-contamination.

Materials from the same depth interval were combined in autoclaved aluminum cylinders with #4 sieve mesh openings at the base to remove gravel-sized soil particles, and homogenized in 4L cylinders using rotation. Table 2 presents the average sample depth, USCS classification, D_{10}, D_{50}, fines content, and water content of the homogenized shallow, middle, deep, and control soil materials. Shallow and middle soil materials had similar grain sizes, fines contents, and water contents, and were from the same material deposit. Deep soil materials, however, consisted of significantly larger grain sizes, contained less fines, and had a higher initial water content. This higher water content agreed with observations during sampling of significant moisture on the outside of samplers below a depth of 11.4 m, potentially due to groundwater capillary rise. Control columns contained commercially manufactured glass beads that ranged between 0.25 and 0.42 mm in diameter and were autoclaved and dry-heat sterilized at 180°C for 3 days prior to column preparation.

Table 2. Soil Material Properties

Sample	Average depth (m)	USCS	D_{10} (mm)	D_{50} (mm)	Percentage finer than #200 sieve	Water content (%)
Shallow	2.0	SP-ML	0.07	0.21	10	3.1
Moderate	5.9	SP-ML	0.08	0.22	9	3.2
Deep	12.0	SP	0.38	1.95	1	6.7
Control	—	SP (glass beads)	0.21	0.30	0	—

Column Preparation

Eight soil columns (two per depth interval and two controls) were prepared in autoclaved Teflon cylinders (69.9-mm ID and 139.7 mm high) with top and bottom caps that allowed for

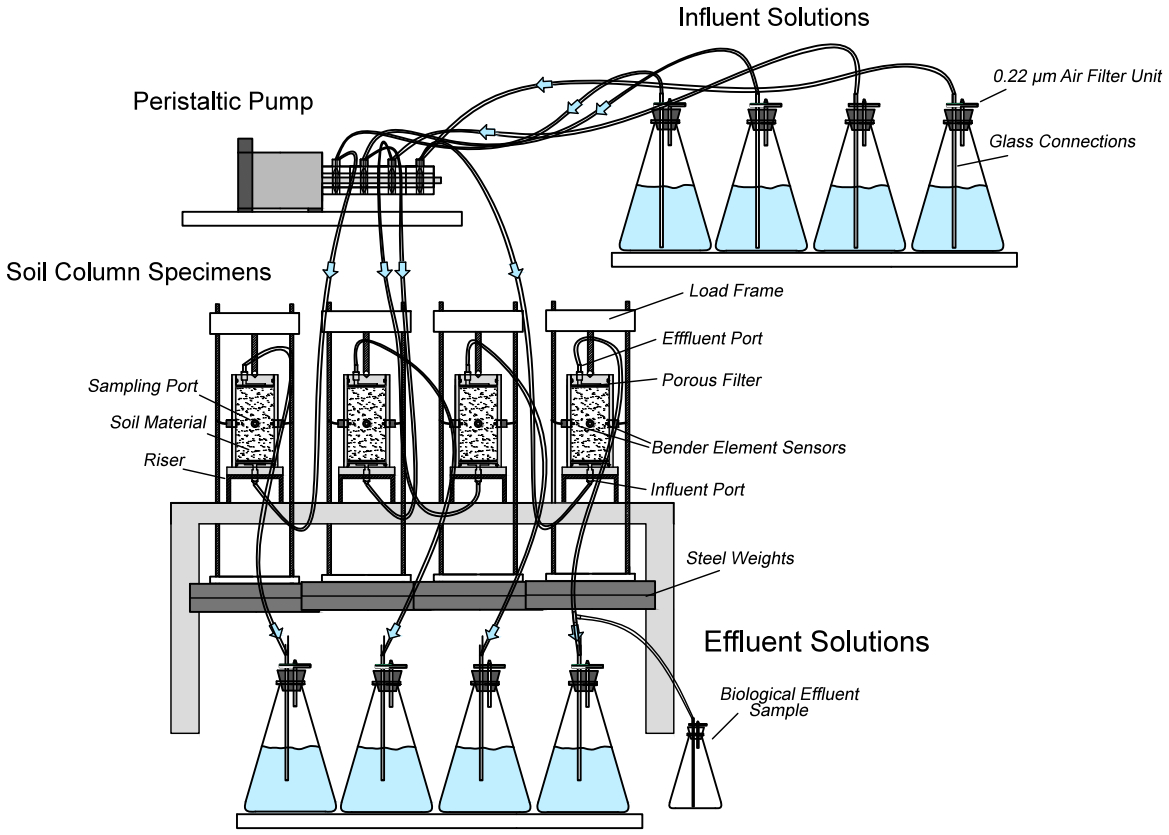

Fig. 2. Soil columns received solution injections from the bottom upward using a treatment solution application system, which included peristaltic pumps and 0.22-μm filters to mitigate potential biological contamination

treatment solution application from the bottom upward. Columns contained two 12.7-mm watertight fittings at midheight for attachment of bender element sensors and a single 3.2-mm septum aqueous sampling port at midheight, perpendicular to bender elements. Plastic filters with pore sizes from 125 to 175 μm (Porex, Fairburn, Georgia) were placed between top and bottom caps and soil materials to minimize soil particulate losses during treatment. Two identical columns were prepared for each depth interval and controls using three soil lifts (approximately 46 mm high) and moist tamping with a sterile steel rod. Initial porosities were 0.32 for both control columns and varied between 0.37 and 0.42 for shallow columns, between 0.34 and 0.37 for middle columns, and between 0.29 and 0.30 for deep columns. An effective stress of 56 kPa was applied to columns through top caps to simulate overburden effective stresses that would be expected at a depth of approximately 5 m within a saturated soil deposit.

Treatment Solutions

Treatment solutions were applied to columns in two treatment phases, stimulation and cementation, using three different solutions with compositions presented in Table 1. The standard stimulation solution was identical to that used in a previous large-scale experiment (Gomez et al. 2016). The enhanced stimulation solution differed by an increase in yeast extract of 0.1 g/L, an increase in NH_4Cl of 87.5 mM, and an initial solution pH adjustment to 9.0. Cementation solutions were similar to standard stimulation solutions but contained soluble calcium concentrations of 250 mM to initiate calcite precipitation. All solutions were filter-sterilized using 0.22 μm vacuum filters (EMD Millipore, Billerica, Massachusetts) after pH adjustment with sodium hydroxide (when applicable). Subaliquotting of filtered treatment solutions into treatment flasks was completed aseptically in a laminar flow hood.

Treatment Application System

Treatment solutions were applied to soil columns using a sterile application system, which used 50-mm 0.22-μm filters (EMD Millipore, Billerica, Massachusetts) for air-displacement and flame-resistant glass connections for sterile exchanging of treatment influent solutions. Fig. 2 shows a schematic of this treatment application system. Solutions were conveyed using autoclaved silicone tubing at a constant flow rate of 25 mL/min using two calibrated peristaltic pumps. Influent treatment solutions were placed in 1-L Erlenmeyer flasks to allow for multiple treatments from the same flask, and injection volumes were determined by measuring changes in flask masses during pumping. During flask exchanging, all exposed glass connections were flame sterilized. Effluent solutions were collected using 2 to 4-L Erlenmeyer flasks with similar air filters to mitigate potential contamination of columns.

Treatment Injections

Table 3 summarizes the stimulation and cementation solution treatment injections for all soil columns. In the first treatment phase, identical columns containing the same material (shallow, middle, deep, and control) received either standard or enhanced stimulation solutions to promote microbial growth and enrich microbial populations capable of urea hydrolysis. Stimulation solution injections of 320 mL (approximately 1.5 PV) were completed once every 23.5 h, with the exception of the first injection, which was retained

Table 3. Summary of Column Treatment Solution Injections

Column material	Stimulation solution type	Stimulation treatments	Cementation treatments
Shallow	Standard	6	14
	Enhanced	4	14
Middle	Standard	8	14
	Enhanced	5	14
Deep	Standard	8	14
	Enhanced	4	14
Control	Standard	11[a]	1
	Enhanced	9[a]	3

[a]Four stimulation treatments were completed following intentional biological contamination.

for 38.5 h to limit initial cell elution. It was hypothesized that columns would require different numbers of stimulation injections before achieving ureolysis rates sufficient to successfully induce calcite precipitation, and that such differences would depend on soil depth and stimulation solution type. In future field-scale treatment applications, it was envisioned that stimulation treatment injections would proceed until a threshold urea hydrolysis rate sufficient to complete calcite precipitation within a specified solution retention time interval was attained. A transition criterion based upon measured urea degradation within the 12-h cementation solution retention period was desired to ensure that all columns had similar ureolysis rates prior to initiating the cementation phase. Previous stimulation experiments involving identical cementation solutions suggested that degradation of approximately 80% of injected urea concentrations within a cementation solution retention period enabled successful biocementation (Gomez et al. 2016). A transition criterion of degradation of 85% or more of the injected urea concentration within 12 h after injection was therefore selected for all soil columns.

Immediately prior to the first cementation solution injection, columns received a 320-mL standard stimulation solution injection to remove anticipated high concentrations of aqueous carbonate species. The reduction of carbonate ions was intended to limit abiotic precipitation of calcite during the initial cementation solution application by reducing solution saturation ratios at the solution-mixing interface (Gomez et al. 2016). During the cementation phase, columns received 320-mL cementation solution injections every 12 h for 7 days (14 total injections), after which treatment ended. Although significant ureolysis in sterile control columns was not detected during sterile stimulation treatments, sterile cementation solution injections were initiated after five and seven stimulation treatments for standard and enhanced control columns, respectively. During the ninth treatment, both control columns were intentionally inoculated at 7–12 cells/mL using effluent solutions from enhanced and standard middle columns at a 1×10^{-6} dilution in stimulation solutions. Intentional inoculation was completed with dilute cell concentrations to assess whether control columns would be sensitive enough to detect low levels of biological contamination if it occurred during the treatment process. If detectable cell growth and/or ureolysis were absent in control columns during the 9-day period of sterile treatments, but were observed following intentional biological contamination, this would suggest that control columns were sensitive to low levels of contamination and that treatments for all columns had been completed in a sterile manner. Following intentional contamination, four sterile standard and enhanced stimulation solution injections were completed for respective control columns to assess cell growth and urea degradation.

Biological Monitoring

Solution volumes of 0.5–1.0 mL were collected aseptically from sampling ports immediately prior to daily treatment applications to monitor total bacterial cell counts in columns. Total direct cell count measurements were completed by the acridine orange staining epifluorescence method of Hobbie et al. (1977) and corrected for blank cell counts using sterile saline solutions. Samples were stored at 4°C for a maximum of 3 h prior to enumeration.

Biogeochemical Monitoring

Additional solution volumes of 1–2 mL were collected before treatment, immediately after treatment, and 1, 2, 4, 6, 8, and 12 h after treatment to monitor temporal changes in aqueous urea concentrations and solution pH. Fluid samples were either measured immediately or frozen for future processing. Solution pH was measured using sample volumes of at least 0.5 mL using an Accumet AB15 pH meter with a semi-micro pH electrode (Thermo Fisher Scientific, Waltham, Massachusetts) that was calibrated daily using a three-point buffer system (4.01, 7.00, and 10.00). Aqueous urea was determined using a colorimetric urea assay modified from Knorst et al. (1997). In the assay, a colorimetric reagent consisting of 4% (weight/volume) p-dimethylaminobenzaldehyde, and 4% (volume/volume) hydrochloric acid in 99.8% ethanol was added to dilute sample volumes and the absorbance (422 nm) was measured using a spectrophotometer.

PHREEQC Geochemical Model

The USGS geochemical program *PHREEQC* was used to verify observed solution pH and urea trends in the standard, enhanced, and cementation solutions using simplified batch reaction calculations. In these calculations, potential effects on solution pH from yeast extract, soil mineral buffering, and residual chemical species from repeated treatments were neglected. Calcite precipitation was modeled as an equilibrium reaction and microbial ureolysis [Eq. (1)] was modeled using a cell-normalized Michaelis–Menten kinetic rate expression following Lauchnor et al. (2015)

$$\frac{d[\text{Urea}]}{dt} = [X]\left(\frac{V_{\max}[\text{Urea}]}{K_m + [\text{Urea}]}\right) \tag{2}$$

where $d[\text{Urea}]/dt$ = ureolysis rate; [Urea] = urea concentration; [X] = ureolytic cell density; $V_{\max}$ = maximum ureolysis rate per cell; and K_m = half-saturation coefficient.

In this batch reaction model, urea hydrolysis was the only kinetically controlled reaction; therefore modeled relationships between urea concentration and solution pH were governed only by equilibrium chemistry and were independent of ureolysis rate. A $V_{\max}$ of 6.4×10^{-9} mmol urea cell^{-1} h^{-1}, K_m of 305 mmol l^{-1}, and total cell density of 5×10^9 cells/mL were selected following estimates of attached and aqueous cell concentrations in column experiments and kinetic parameters reported by Lauchnor et al. (2015) for *S. pasteurii*.

Shear-Wave Velocity Measurements

Biocementation of granular soils has been shown to result in significant increases in soil small-strain shear stiffness, $G_{\max}$ (e.g., DeJong et al. 2006, 2009, 2010; Martinez et al. 2013; Montoya et al. 2013; Montoya and DeJong 2015; Gomez et al. 2016). Shear-wave velocity (V_s) measurements, therefore, provide an effective method for nondestructive real-time monitoring of

cementation progression. V_s measurements were completed using piezoelectric bender element sensor pairs (Piezosystems, Woburn, Massachusetts) assembled following Montoya et al. (2012) and protected from the high-conductivity aqueous environment using a multistep coating process. Bender elements were first coated with Hysol epoxy adhesive (Loctite, Henkel Adhesives North America, Rocky Hill, Connecticut) followed by a thin coating of electronics wax (Vishay Precision, Malvern, Pennsylvania) and electronics insulation coating (GC Electronics, Rockford, Illinois) to provide a durable waterproof barrier. Prior to placement, bender elements were sterilized with a 40-min exposure to 10% (volume/volume) bleach solution and were rinsed using five consecutive 5-min washes in 70% ethanol to remove residual bleach. Sensor tip-to-tip spacing distances were determined in a sterile manner by obtaining images of assembled columns before soil placement and completing subsequent image analysis with *ImageJ* software (Schneider et al. 2012). V_s measurements were completed a minimum of once daily, during which bender element transmitters were excited using a 24 V 100-Hz square wave generated by a signal generator and data acquisition system (NI cDAQ-9174, National Instruments, Austin, Texas), and received signals were measured and recorded with an oscilloscope (Picoscope 5243B, Pico Technology, Tyler, Texas) at a sampling frequency of 2 MHz. V_s values were determined from visual interpretation of S-wave arrivals and known sensor-spacing distances.

Unconfined Compressive Strength Measurements

Unconfined compressive strength (UCS) measurements were completed on extruded soil columns posttreatment in accordance with ASTM D2166 (ASTM 2013). Prior to extrusion, columns were placed in a drying oven at 100°C for 14 days. Posttreatment rinsing of soil columns was not completed prior to specimen drying in order to avoid potential dissolution of microbial impressions and calcite microstructures, which were of interest in this study. Although precipitation of soluble salts such as ammonium chloride from residing effluent solutions was anticipated during the drying process, only small amounts of salt were observed on the outside of columns after drying and were not expected to influence measured soil strengths. Soil columns were extruded using a hydraulic jack using pressures of less than 100 kPa. Following extrusion, columns were sulfur-capped on the ends to allow for even application of compressive stresses. During testing, a constant rate of axial strain of 1% per min was used, and displacements and loads were electronically recorded with a GeoJac (Bellaire, Texas) data acquisition system and software.

Calcite Content Measurements

Following failure of columns during UCS testing, columns were partitioned along their length into four discrete 2.8-cm segments for calcite content (weight/weight) measurements, oven dried, and homogenized to yield representative subsamples. Calcite content was quantified in accordance with ASTM D4373 (ASTM 2014) by reacting calcite with hydrochloric acid to generate carbon dioxide gas and a corresponding increase in pressure in a test chamber. Calibration relationships between chamber pressure and calcite masses (98.0–100.5% by mass, Fisher Scientific, Waltham, Massachusetts) were used to determine soil sample calcite contents from observed chamber pressures. A minimum of three measurements were performed per discrete column segment to assess repeatability.

Scanning Electron Microscope Imaging

Scanning electron microscope images were completed with a Hitachi S-4100 (Tarrytown, New York) field emission scanning electron microscope using an acceleration voltage of 2 kV and a magnification of 5000×. Prior to imaging, soil specimens were oven dried for an additional 5 days and mounted to imaging pedestals using carbon tape.

Results

Solution Optimization

Fig. 3 shows results from solution optimization experiments, including urea concentration measurements in time for select batch [Fig. 3(a)] and soil column experiments [Fig. 3(b)]. Fig. 3(a) shows urea concentrations over time for batch experiments completed using shallow, middle, and deep soil materials treated with either the standard stimulation solution or a similar modified A stimulation solution which had yeast extract concentrations that were 10 times higher (1.0 g/L YE). Batch experiments were completed in duplicates; however, significant variations in ureolysis rates between replicates were observed. Replicates with the highest urea degradation over the monitoring interval are presented, representing the most favorable stimulation results. Significantly slower ureolysis rates were observed for all batch specimens compared with soil columns and were attributed to large solution-to-soil ratios and single treatments, which do not provide additional nutrients or remove metabolic waste. In all batch specimens regardless of depth, total cell densities converged to values near 10^8 cells/mL and 10^9 cells/mL after 3 and 4 days in standard and modified A

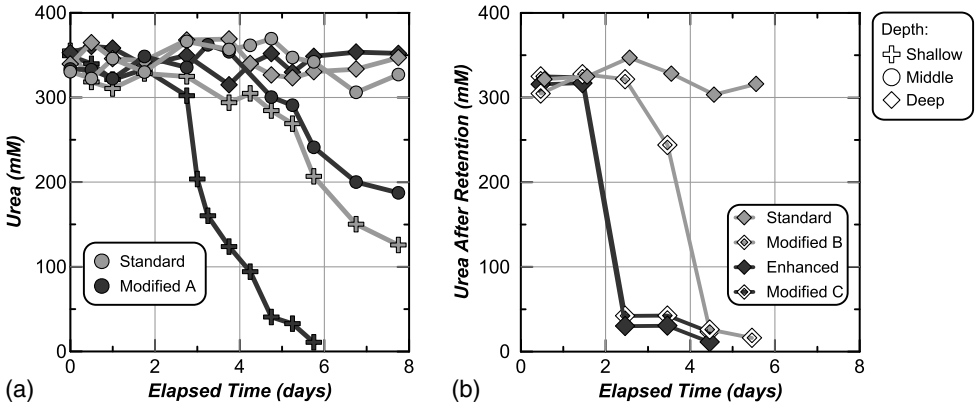

Fig. 3. Urea concentration measurements for solution optimization: (a) batch; (b) soil column experiments versus elapsed treatment time

J. Geotech. Geoenviron. Eng., 2018, 144(1): 04017098

specimens, respectively (data not shown). In addition, solution pH increased to values above approximately 9.0 for all specimens within the 8-day monitoring period (data not shown). Despite similar total cell densities and solution pH values between batch specimens, urea degradation exceeding 50 mM was only observed in shallow batch specimens and the modified A middle specimen over the monitoring period. In shallow batch specimens, faster urea degradation occurred in the modified A specimen, with approximately 200 mM of urea degraded approximately 4 days earlier than in the standard solution specimen. The absence of detectable urea degradation in both deep specimens and the standard middle specimen prompted a second batch experiment using similar stimulation solutions with initial solution pH values of 7.0, 8.0, and 9.0, and higher urea degradation was observed for all depths in the most alkaline pH 9.0 specimens (data not shown).

A subsequent soil column experiment was completed using deep soil material to evaluate the effect of increased NH_4Cl and YE concentrations, in conjunction with adjustment of initial solution pH to 9.0. In these experiments, YE concentrations were limited to 0.2 g/L to avoid providing more organic matter than could be aerobically respired at depth. If excess YE were provided, it was hypothesized that anaerobic fermentation could result in the production of organic acids that would compromise both ureolytic enrichment and achieved calcite precipitation. The upper-bound YE concentration of 0.2 g/L was estimated after assuming a treatment solution dissolved oxygen concentration of 7.8 mg/L, a yeast extract carbohydrate content of 117 mg/g, and 40% aerobic respiration and 60% assimilation of YE carbohydrates. Fig. 3(b) presents urea concentrations following solution retention periods of approximately 23.5 h versus time for four columns treated with either the standard stimulation solution or with modified B, enhanced, or modified C solutions which included 0.2 g/L YE, had an initial solution pH of 9.0, and had NH_4Cl concentrations of 12.5 mM (standard concentration), 100 mM, or 200 mM. In the standard solution column, no significant urea degradation was observed within the 6-day monitoring period. For all columns with YE concentrations of 0.2 g/L and initial solution pH adjustment to 9.0, however, nearly full urea degradation was observed, although at different times dependent on NH_4Cl additions. The modified B column with the standard NH_4Cl concentration of 12.5 mM resulted in nearly full ureolysis of the injected urea concentration during the fifth treatment retention period. For the enhanced and modified C columns with NH_4Cl additions of 100 and 200 mM however, complete ureolysis occurred during the third treatment retention period, suggesting that stimulation time was relatively insensitive to NH_4Cl additions above 100 mM.

Biological Monitoring

Fig. 4 presents aqueous total cell densities for all columns versus elapsed treatment time. Immediately following initial saturation with stimulation solutions at the start of treatment, shallow, middle, and deep soil columns had similar aqueous total cell densities ranging from 1 to 5×10^4 cells/mL. Twenty-one hours after the first stimulation treatment, shallow and middle columns had similar densities between 1×10^4 cells/mL and 1×10^5 cells/mL; however, deep columns had significantly higher aqueous cell densities between 4×10^6 cells/mL and 6×10^7 cells/mL. After three additional days, aqueous total cell densities for shallow, middle, and deep columns converged to values between 1×10^7 cells/mL and 1×10^8 cells/mL and remained at these similar values during stimulation. During cementation, however, aqueous total cell densities for a given column decreased by approximately one order of magnitude and columns converged to values between

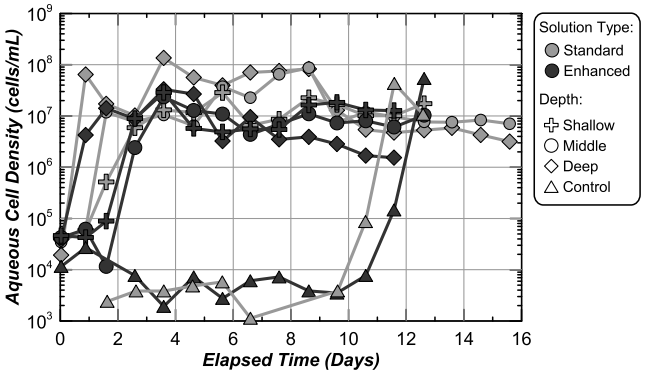

Fig. 4. Aqueous cell densities measured immediately before treatment solution application versus elapsed treatment time for all soil columns

1×10^6 cells/mL and 2×10^7 cells/mL. For sterile control columns, aqueous total cell densities generally ranged from 1×10^3 cells/mL to 1×10^4 cells/mL, consistent with densities observed from background contamination in sterile blank cell counts. Following intentional contamination of control columns completed during the ninth treatment injection, aqueous cell densities increased to approximately 5×10^7 cells/mL after three and 4 days in the standard and enhanced control columns, respectively.

Biogeochemical Monitoring

Fig. 5 presents aqueous urea concentrations measured in shallow, middle, and deep columns versus time following all stimulation

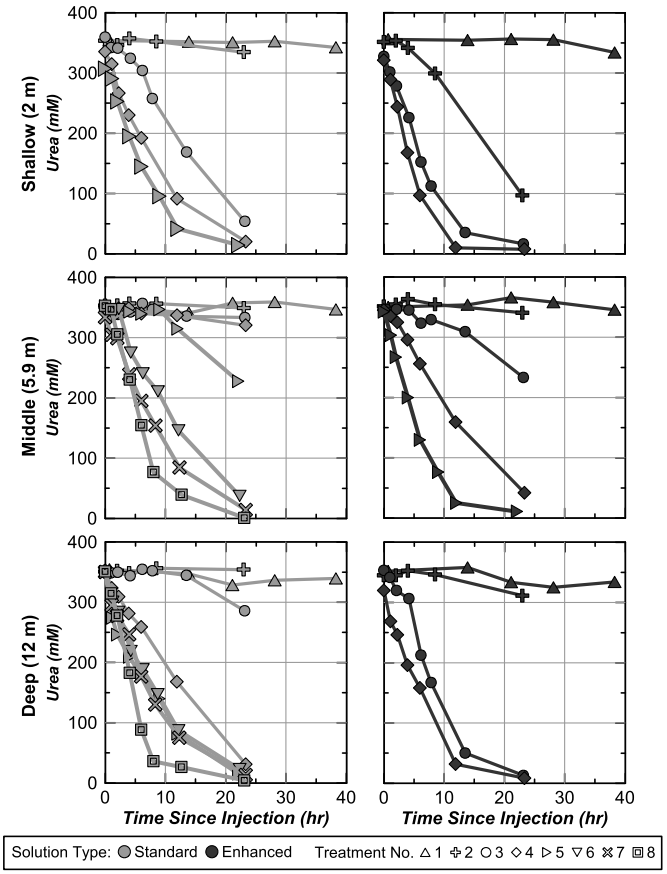

Fig. 5. Urea concentration measurements for all shallow, middle, and deep columns versus time since injection for all stimulation solution retention periods

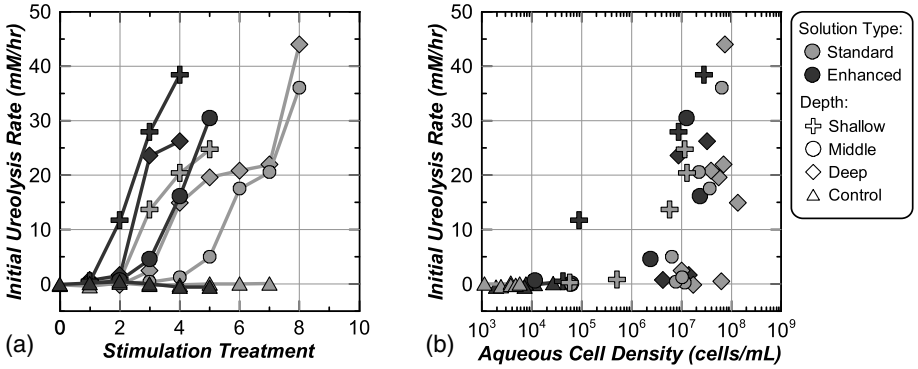

Fig. 6. Initial ureolysis rates for all columns versus (a) stimulation treatment number; (b) aqueous total cell density

treatment injections. For the first stimulation treatment retention period, almost no urea degradation was observed during 38.5 h in any column. During the second treatment retention period however, the onset of urea hydrolysis and approximately 250 mM of urea degradation was observed in the enhanced shallow column. Within the third treatment retention period, the onset of urea hydrolysis and urea degradation exceeding 300 mM was detected in both the standard shallow and enhanced deep columns. During the fourth treatment retention period, the onset of urea hydrolysis and urea degradation exceeding 300 mM was detected in both the enhanced middle and standard deep columns. Finally, the slowest onset of urea hydrolysis and urea degradation exceeding 300 mM occurred in the standard middle column during the sixth treatment retention period. Following the onset of detectable urea hydrolysis, urea degradation magnitudes and rates increased with further stimulation treatments for all columns. Urea degradation in excess of 250 mM during a treatment retention period occurred in enhanced columns, 1, 2, and 1 days earlier for shallow, middle, and deep materials, respectively, compared with standard columns. Although measurements for control columns are not presented, urea concentrations remained near 350 mM for all times except 4 days following intentional contamination, when urea degradation of 200 and 60 mM was detected in the enhanced and standard control columns, respectively.

Initial ureolysis rates were estimated from urea measurements within the concentration range of 350 mM (injected concentration) to 50 mM during a given retention period for all columns during stimulation. These initial rate estimations approximate that urea concentrations decreased in time following a linear trend (zeroth-order kinetics) and minimized potential increases in rates from cell growth and potential decreases in rates from urea concentrations below anticipated whole cell zeroth-order ranges (Lauchnor et al. 2015). Fig. 6(a) presents initial ureolysis rates for all columns as a function of stimulation treatment number. As shown, initial ureolysis rates increased for all nonsterile columns with further stimulation treatments. For columns containing soil material from the same depth, initial ureolysis rates for columns treated with the enhanced solution were higher than those for columns treated with standard solutions for all treatments. The more rapid urea degradation observed for enhanced columns resulted in the satisfaction of the 12-h treatment phase transition criterion 1, 3, and 4 days earlier for shallow, middle, and deep columns, respectively. For the same stimulation solution type, initial ureolysis rates followed a consistent order by material depth, with shallow columns exhibiting the highest ureolysis rates, deep columns exhibiting the second-highest rates, and middle columns exhibiting the lowest rates for each stimulation treatment. Initial ureolysis rates were also determined from urea measurements completed during cementation and indicated further increases in ureolysis rates to values ranging from 81 to 104 mM/h during the last cementation treatment (data not shown). Initial ureolysis rates for control columns remained near 0 mM/h for all sterile stimulation treatments. Fig. 6(b) presents initial ureolysis rates during stimulation versus aqueous total cell densities at the end of a given retention period for all columns. Following the first stimulation treatment, aqueous total cell densities in shallow, middle, and deep columns ranged from 1×10^4 cells/mL to 1×10^6 cells/mL; however, no significant ureolysis rates were observed. As aqueous total cell densities in middle and deep columns approached 1×10^7 cells/mL to 1×10^8 cells/mL, a wide range of initial ureolysis rates from 0 to 44 mM/h were observed at nearly constant total cell counts. In shallow columns, however, increases in aqueous total cell densities to values near 1×10^7 cells/mL to 1×10^8 cells/mL resulted immediately in significant ureolysis rates.

Fig. 7 presents measurements of aqueous urea concentrations versus corresponding solution pH measurements for all columns for all measurement times by treatment solution type. *PHREEQC*-modeled solution pH and urea concentration values are also provided for comparison. Relationships between urea concentration and solution pH were governed by treatment solution chemical composition and therefore all other factors, including soil material type and temporal differences, are not indicated. Following stimulation solution applications, standard and enhanced solution columns had pH values near 7.8 and 9.0, respectively, prior to the occurrence of significant ureolysis. Both standard and enhanced

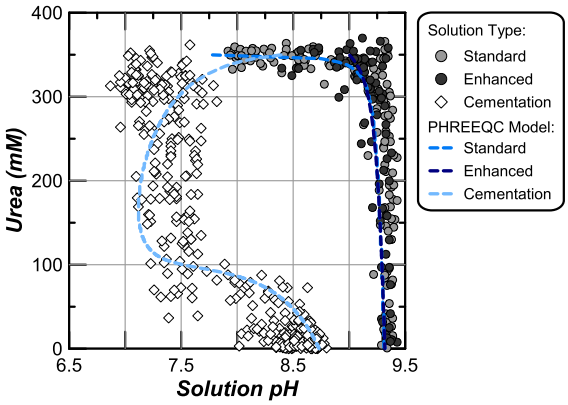

Fig. 7. Corresponding urea concentration and solution pH measurements for standard stimulation, enhanced stimulation, and cementation solutions for all soil columns and measurement times with *PHREEQC* batch reaction modeling results

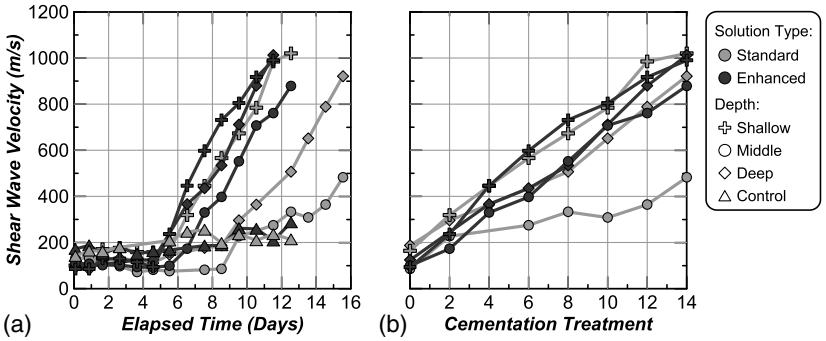

Fig. 8. Shear-wave velocity measurements versus (a) elapsed treatment time; (b) cementation treatment number for all soil columns

stimulation solution columns, however, experienced significant pH increases following urea degradation of approximately 15 mM with the majority of urea hydrolysis occurring over a narrow band of solution pH values between 9.2 and 9.4. During cementation, observed solution pH and urea trends were not significantly influenced by whether or not columns had received standard or enhanced stimulation solutions previously. In all columns during cementation, initial urea degradation of approximately 250 mM was observed within a narrow band of solution pH values from approximately 7.0 to 7.7. After urea concentrations were reduced below approximately 100 mM during cementation, however, large increases in solution pH were observed in all columns, with values generally between 8.3 and 8.8 after completion of urea hydrolysis. *PHREEQC* batch reaction modeled relationships between urea concentration and solution pH agreed well with observed experimental trends for all three treatment solutions.

Shear-Wave Velocity

Fig. 8(a) plots shear-wave velocity measurements for all columns versus elapsed treatment time. Initial V_s values varied between 85 and 131 m/s for shallow, middle, and deep columns, whereas higher initial V_s values between 150 and 170 m/s were measured for glass bead control columns. For a given soil depth, initial V_s values did not vary by more than 20 m/s between standard and enhanced columns. Following treatment, final V_s values were 1,020 and 990 m/s for shallow columns, 483 and 879 m/s for middle columns, and 921 and 1,013 m/s for deep columns for standard and enhanced stimulation solutions, respectively. The V_s increases occurred over different 7-day periods for all columns due to differences in when the measured urea degradation exceeded the treatment phase transition criterion and cementation was initiated. Fig. 8(b) plots shear-wave velocity measurements for shallow, middle, and deep columns versus number of cementation treatments. Linear rates of V_s increase per cementation treatment were determined for all columns during this period and were between 50 and 65 m/s per treatment for all columns with the exception of the standard middle specimen, which had a lower V_s increase of approximately 25 m/s per treatment. Although large increases in V_s were not observed in control columns, small increases in V_s in these columns are attributed to small amounts of abiotic calcite precipitation from sterile cementation solution injections.

Unconfined Compressive Strength

Fig. 9 presents axial strain and stress measurements for shallow, middle, and deep columns during UCS testing. Measurements are presented following the application of a 50-kPa seating stress, after which stress increases were applied. Unconfined compressive

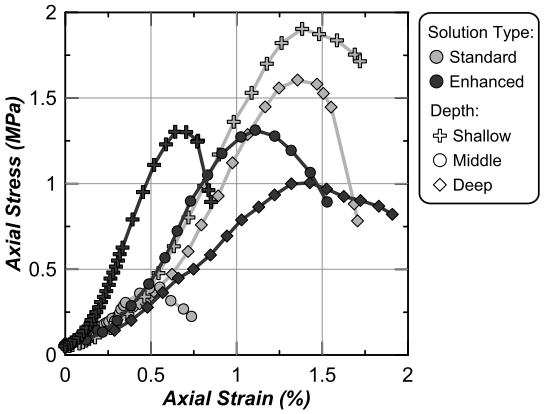

Fig. 9. Axial stress versus axial strain measurements for all soil columns during unconfined compressive strength testing

strength measurements were not obtained for control columns due to a lack of cementation in these columns. During initial loading of cemented soil columns, low initial axial stiffnesses were observed and attributed to the closing and sealing of microcracks in columns that could have developed during the extrusion process and the compression of looser materials existing at column ends. Following this initial loading region, at axial strains from 0.12 to 0.25%, column axial stiffnesses appeared to increase significantly and remained relatively linear until cementation failure occurred and a peak axial strength (UCS) was observed. The UCS values ranged between 1.9 and 1.3 MPa for shallow columns, 0.4 and 1.3 MPa for middle columns, and 1.6 and 1.0 MPa for deep columns, for standard and enhanced solutions, respectively.

Calcite Content Distributions

Fig. 10 presents average calcite contents by mass for all discrete column sections versus distance from column injection locations, i.e., the bottom of columns. Error bars indicate one standard deviation above and below average calcite content values computed for discrete sections using three measurements. Calcite contents for shallow columns were similar across the entire soil column length, with average calcite contents gradually decreasing from approximately 8–10% by mass near the bottom injection location to 3–5% by mass near the top of columns. Calcite contents for middle columns differed substantially in the bottom three-fourths of columns, with the standard middle column achieving much lower calcite contents. Average calcite contents for middle columns ranged from approximately 7–10.5% by mass near the bottom injection location to

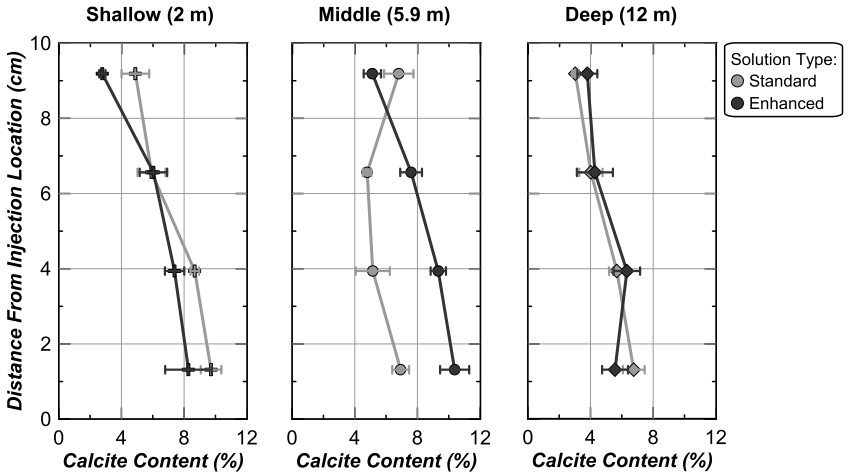

Fig. 10. Average calcite contents by mass for discrete column sections versus distance from column injection locations for all shallow, middle, and deep columns with standard deviations of measurements indicated by error bars

5–7% by mass near the top of columns. Calcite contents for deep columns were similar across the entire column length, with average calcite contents of approximately 5.5–7% by mass near the bottom injection location and modest reductions in calcite content to 3–4% near the top of columns.

Scanning Electron Microscope Images

Scanning electron microscope images of cemented soil samples obtained at midheight along columns were completed following testing. Figs. 11(a–f) present SEM images of calcite crystals on sand particle surfaces for all columns completed at 5000× magnification. Bacterial cell impressions were observed on calcite crystals from all columns regardless of material depth and stimulation solution type. Impressions varied in size and morphology between columns; however, in general, rod-shaped impressions varied in length between 2 and 4 μm, with diameters near 0.5 μm, and coccus-shaped impressions were observed with diameters between 0.5 and 0.75 μm. Although small subsamples cannot be fully representative of all locations within a given column, differences in impression morphology may reflect the microbial diversity expected in stimulated soil columns during biocementation.

Discussion

Solution optimization experiments demonstrated that the standard stimulation solution, used in previous experiments with success, may be not be optimal for stimulation of ureolytic microorganisms in soil materials at depths exceeding 5 m. Poor stimulation of ureolysis observed in deeper soil materials treated with the standard stimulation solution is attributed to limited selection for alkaliphilic ureolytic bacteria and greater utilization of substrates by competing nonureolytic and/or nonalkaliphilic ureolytic bacteria. It was hypothesized that ureolytic stimulation could be improved in deeper soil materials containing fewer ureolytic cells or spores initially if selective environmental conditions were imposed to limit growth of competing microorganisms. Further solution optimization experiments were completed to assess the potential of stimulation solutions with higher initial pH and ammonium concentrations to impose additional selective pressure that favored alkaliphilic and ammonium-tolerant microorganisms, of which a greater fraction were anticipated to be ureolytic. An enhanced stimulation solution was identified that improved stimulation of ureolysis in deeper soil

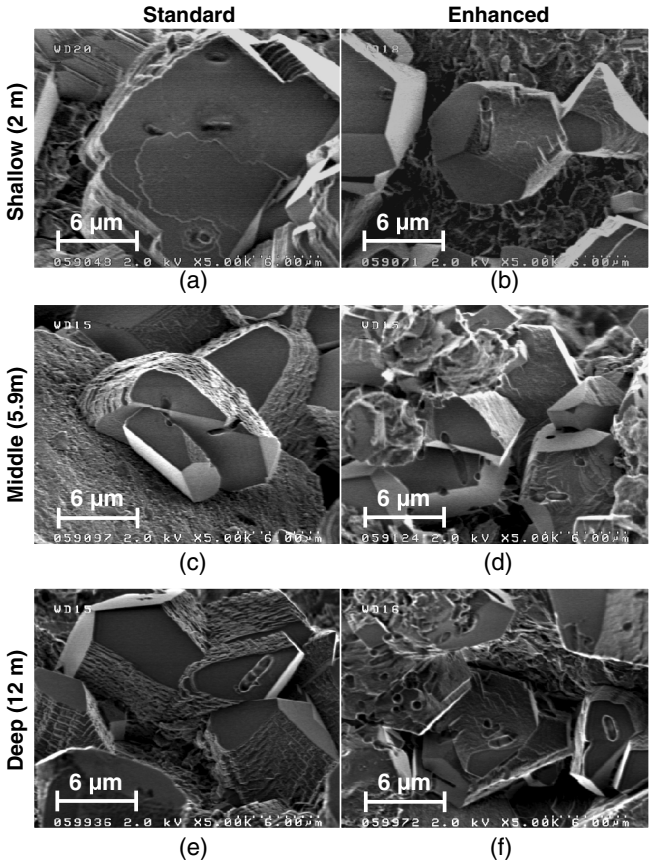

Fig. 11. Scanning electron microscope images of microbial impressions on calcite crystals at 5000× for (a) standard and (b) enhanced shallow specimens; (c) standard and (d) enhanced middle specimens; (e) standard and (f) enhanced deep specimens

materials using 0.2 g/L YE, initial solution pH adjustment to 9.0, and an NH_4Cl concentration of 100 mM. Although further parametric tests are needed, the enhanced stimulation solution represents a preliminary optimization of several treatment constituents that may control biostimulation of ureolytic bacteria in natural soil materials.

J. Geotech. Geoenviron. Eng., 2018, 144(1): 04017098

In the second experiment, ureolytic stimulation feasibility with depth was assessed using soil materials obtained at three depths and treated with standard or enhanced stimulation solutions. For all material depths, the use of the enhanced stimulation solution resulted in higher ureolysis rates at similar times and therefore reduced the number of stimulation treatments required for shallow, middle, and deep columns by 1, 3, and 4 treatments, respectively. After considering reductions in required standard stimulation treatments, the 87.5-mM-higher ammonium concentration included in the enhanced solution, and assuming a solution total ammonium production of twice the urea concentration by reaction stoichiometry [Eq. (1)], the use of the enhanced solution was estimated to reduce produced ammonium by 4.7, 22.0, and 32.3 kg/m^3 of treated soil for the shallow, middle, and deep materials, respectively. Although potential reductions in ammonium by-products will be dependent on biological aspects of treated soil materials and particular treatment injection schemes, the reduction of total ammonium in this study through the use of the enhanced solution is promising.

For shallow columns, aqueous total cell densities were similar in time, suggesting that stimulation solution differences did not significantly affect total cell growth. When total cell densities exceeded 1×10^6 cells/mL in both shallow columns, however, initial ureolysis rates increased significantly and were measured as high as 14 and 28 mM/h for standard and enhanced columns, respectively. This immediate increase in initial ureolysis rates to nonzero values following the onset of significant total cell growth was not observed for middle and deep columns. The apparent correlation between increases in total cell densities and increases in ureolysis rates in the shallow material, suggests that initial microbial populations in these surficial materials may have had a higher fraction of ureolytic microorganisms compared with other depths. Following cementation, no significant differences in geotechnical improvement relating to stimulation solution type were observed between shallow columns. Final V_s measurements between columns differed by 3%, UCS values differed by 31%, and average calcite content distributions differed by no more than 2% by mass at any measurement location. In all soil columns, a cementation gradient was observed across column lengths, with the largest calcite contents observed near the injection location. Reductions in calcite content with distance from the injection port in all columns were attributed to calcite precipitation reactions occurring during injections due to solution mixing and/or urea hydrolysis.

For middle columns, relatively similar aqueous total cell densities were observed over time, with slightly faster initial cell growth occurring in the standard solution column. Compared with shallow or deep materials treated with the same stimulation solution at similar times, initial ureolysis rates were the lowest for both middle columns. In addition, increases in total cell densities in middle and deep material columns did not appear to result in immediate increases in initial ureolysis rates. Instead, significant increases in urea degradation were observed while maintaining similar total aqueous cell densities, suggesting that microbial populations in middle and deep materials may have required continued enrichment to achieve significant increases in ureolytic activity. When comparing geotechnical improvement between middle columns, consistently lesser improvement was observed in the standard middle column despite identical cementation treatments and similar ureolysis rates prior to cementation. In the standard middle column, final V_s values were 45% lower, UCS was 69% lower, and average calcite contents in the bottom three-fourths of columns were approximately 3–4% by mass lower. Reductions in calcite precipitation and geotechnical improvement in the standard middle column may have resulted from the enrichment of a significantly different and less favorable microbial population in this column due to reduced selective pressure for ureolytic microorganisms in the standard solution. The standard middle column had the lowest urea degradation rate during stimulation of all tested columns despite having the fastest total cell growth of all shallow and middle columns. In addition, visual observations during total cell counts for the standard middle column indicated the presence of distinctly different small coccus-shaped bacterial cells, compared with other columns, which generally contained rod-shaped bacterial cells. In mixed microbial communities, differences in stimulated ureolytic and nonureolytic microbial populations may alter local biogeochemical conditions near soil particles, affecting cementation distribution and magnitude, despite not being reflected in bulk aqueous measurements (e.g., acidifying anoxic microsites).

For deep columns, similar aqueous total cell densities were observed between standard and enhanced columns. Although initial cell counts between all soil columns were comparable immediately after saturation, 21 h into the first stimulation retention period, total cell densities in deep columns were approximately 1×10^2 cells/mL to 1×10^3 cells/mL higher than in all other columns. During stimulation, urea degradation rates in deep columns also exceeded middle-material columns treated with identical stimulation solutions. The more rapid initial total cell growth and higher ureolysis rates observed in deep columns versus middle columns suggest that significant and unexpected biological differences existed between these soil materials. Significantly higher water contents and observations of moisture during sampling suggest that the deep material may have been influenced by the groundwater table. Groundwater introduced from nearby Cache Creek may have allowed microorganisms to remain metabolically active by providing nutrients and water that may not have been present in shallow or middle materials. When comparing final geotechnical improvement between deep columns, no consistent trends relating to stimulation solution type were observed. Final V_s measurements between columns differed by 9%, UCS values differed by 38%, and calcite content distributions differed by no more than 1% by mass at any measurement location.

During sterile treatments, control columns maintained total cell densities similar to sterile solution blanks, suggesting that mitigation of biological contamination from solution applications was successful. Four days after intentional biological contamination, significant urea degradation and total aqueous cell densities near 5×10^7 cells/mL were measured in both control columns. Detectable cell growth and ureolysis resulting from intentional contamination of control columns suggest that if similarly low levels of contamination had occurred during treatment applications, total cell density and urea measurements would have reflected such contamination within the 9-day duration of sterile treatments.

Although it was hypothesized that adjustment of initial pH to 9.0 would limit the ability of solution pH monitoring to capture changes in urea degradation in the enhanced solution, results for both standard and enhanced stimulation solution columns suggested that solution pH alone cannot be used to quantitatively assess urea degradation. In both the standard and enhanced solutions, nearly all urea degradation exceeding approximately 15 mM was observed at constant solution pH values near 9.3. The inability of solution pH changes in the tested stimulation solutions to capture increases in urea degradation can be attributed to the low initial buffering capacity of these solutions, which permits large solution pH changes following little urea degradation. *PHREEQC* modeling results confirmed experimental observations and indicated that small amounts of urea degradation near the 15 mM observed would be sufficient to induce large solution pH changes from approximately 7.3 to approximately 9.0 in the standard stimulation solution

for a single treatment. It is likely that residual total ammonium and hydroxide concentrations in soil columns during repeated treatments, however, would require increasingly less urea degradation to achieve similar pH changes due to ammonium buffering. Despite this simplification, the modeled results also indicated that in both stimulation solutions, significant urea degradation would occur at a nearly constant solution pH of approximately 9.3 due to increasing proportions of produced NH_3 remaining as NH_3 at higher solution pH values (pKa of $NH_3/NH_4^+ = 9.24$), decreasing hydroxide production and solution pH increase.

During cementation, solution pH also did not appear to effectively indicate urea degradation because nearly constant solution pH values between 7.0 and 7.7 were observed during urea degradation from 350 to approximately 100 mM. It was hypothesized that the absence of significant solution pH changes during the initial urea degradation of approximately 250 mM resulted from the simultaneous production of protons from calcite precipitation and hydroxide ions from urea hydrolysis. During calcite precipitation, the production of protons occurs when carbonate ions are consumed and existing carbonic acid and bicarbonate species speciate to replace carbonate ions. Once urea concentrations were reduced to approximately 100 mM, however, large increases in cementation solution pH values from approximately 7.5 to approximately 8.5 were observed. Significant increases in solution pH at low urea concentrations were therefore attributed to reductions in soluble calcium, the absence of calcite precipitation, and all remaining urea hydrolysis contributing to solution pH rise. Batch reaction modeling results for the cementation solution were similar to experimental trends and confirmed that the immediate increase in solution pH from approximately 7.4 to approximately 8.7 occurred when calcium concentrations were less than 5 mM and calcite precipitation was minimal (data not shown). Although solution pH monitoring cannot quantitatively assess urea degradation in the standard, enhanced, and cementation solutions, experimental and geochemical modeling results suggest that this monitoring method may be used to indirectly determine the end of calcite precipitation reactions when calcium is the limiting precipitation reactant and excess urea is present.

Conclusions

Although the effect of groundwater chemistry, soil water saturation, and various other site-specific conditions on ureolytic stimulation were not examined, the biological, chemical, and geotechnical results of this study suggest that native ureolytic microorganisms may be successfully stimulated in natural soil deposits to induce calcite precipitation at treatment depths up to 12 m for geotechnical ground improvement applications. Following solution optimization experiments, an enhanced stimulation solution was identified which improved ureolytic stimulation through ammonium chloride and yeast extract additions and alkaline solution pH adjustment. A sterile sampling and column testing program was completed using soil materials obtained at shallow (2 m), middle (5.9 m), and deep (12 m) depths from a geotechnical boring to assess ureolytic stimulation feasibility and differences between standard and enhanced stimulation solutions. Despite similar total cell growth between columns, significant differences in stimulated urea degradation were observed between soil depths and stimulation solution types in time. For the same soil depth, initial ureolysis rates for enhanced solution columns exceeded standard solution columns for all stimulation treatments. Ureolysis rates also followed a consistent order for the same stimulation solution type by material depth, with shallow columns exhibiting the highest ureolysis rates followed by deep and middle columns, respectively. Higher ureolysis rates observed in deep columns than in middle columns were attributed to the influence of the groundwater table, which may have increased water and nutrient availability for microorganisms. Following 14 cementation treatments, cemented soil columns achieved similar final shear-wave velocities, unconfined compressive strengths, and calcite content distributions, with the exception of the standard middle column specimen, which had significantly less improvement. Although the lesser improvement obtained in the standard middle column specimen requires further investigation, differences in stimulation solution type did not appear to consistently result in significant differences in final geotechnical improvement. Enhanced stimulation solutions may allow for stimulation of native ureolytic microorganisms at field-scale treatment depths with potential reductions in treatment time, material utilization, and environmental impacts associated with ureolytic MICP ground improvement compared with previous stimulation and augmentation treatment approaches.

Acknowledgments

This material is based upon work supported by the National Science Foundation grants CMMI-1539774 and CMMI-1234367, and by the Engineering Research Center Program of the National Science Foundation under NSF Cooperative Agreement No. EEC-1449501. Any opinions, findings, and conclusions or recommendations expressed in this material are those of the authors and do not necessarily reflect the views of the National Science Foundation. The authors also thank Gabby Hernandez, Alexandra San Pablo, Kevin Kuei, and Andreas Gavras of the University of California, Davis for their assistance with the project and Teichert Aggregates Woodland for providing access to and support with the project testing location.

References

Acea, M. J., Moore, C. R., and Alexander, M. (1988). "Survival and growth of bacteria introduced into soil." *Soil Biol. Biochem.*, 20(4), 509–515.

Armon, R., and Arbel, T. (1998). "Indigenous soil microflora versus introduced microorganisms in subsurface bioremediation." *Soil and aquifer pollution*, Springer, Berlin, 149–158.

ASTM. (2013). "Standard test method for unconfined compressive strength of cohesive soil." *ASTM D2166/D2166M-13*, West Conshohocken, PA.

ASTM. (2014). "Standard test method for rapid determination of carbonate content of soils." *ASTM D4373-14*, West Conshohocken, PA.

Atlas, R., and Bartha, R. (1973). "Stimulated biodegradation of oil slicks using oleophilic fertilizers." *Environ. Sci. Technol.*, 7(6), 538–541.

Bang, S., Min, S., and Bang, S. (2011). "Application of microbiologically induced soil stabilization technique for dust suppression." *Int. J. GeoEng.*, 3(2), 27–37.

Burbank, M., Weaver, T., Green, T., Williams, B., and Crawford, R. (2011). "Precipitation of calcite by indigenous microorganisms to strengthen liquefiable soils." *Geomicrobiol. J.*, 28(4), 301–312.

Burbank, M., Weaver, T., Lewis, R., Williams, T., Williams, B., and Crawford, R. (2013). "Geotechnical tests of sands following bioinduced calcite precipitation catalyzed by indigenous bacteria." *J. Geotech. Geoenviron. Eng.*, 10.1061/(ASCE)GT.1943-5606.0000781, 928–936.

DeJong, J. T., et al. (2009). "Upscaling of bio-mediated soil improvement." *Proc., 17th Int. Conf. on Soil Mechanics and Geotechnical Engineering*, Millpress Science, Rotterdam, Netherlands, 2300–2303.

DeJong, J. T., et al. (2013). "Biogeochemical processes and geotechnical applications: Progress, opportunities and challenges." *Géotechnique*, 63(4), 287–301.

DeJong, J. T., Fritzges, M., and Nüsslein, K. (2006). "Microbial induced cementation to control sand response to undrained shear." *J. Geotech.*

Geoenviron. Eng., 10.1061/(ASCE)1090-0241(2006)132:11(1381), 1381–1392.
DeJong, J. T., Mortensen, B. M., Martinez, B. C., and Nelson, D. C. (2010). "Bio-mediated soil improvement." *Ecol. Eng.*, 36(2), 197–210.
Eilers, K., Debenport, S., Anderson, S., and Fierer, N. (2012). "Digging deeper to find unique microbial communities: The strong effect of depth on the structure of bacterial and archaeal communities in soil." *Soil Biol. Biochem.*, 50, 58–65.
Fierer, N., Schimel, J., and Holden, P. (2003). "Variations in microbial community composition through two soil depth profiles." *Soil Biol. Biochem.*, 35(1), 167–176.
Fujita, Y., et al. (2008). "Stimulation of microbial urea hydrolysis in groundwater to enhance calcite precipitation." *Environ. Sci. Technol.*, 42(8), 3025–3032.
Fujita, Y., Ferris, F. G., Lawson, R. D., Colwell, F. S., and Smith, R. W. (2000). "Calcium carbonate precipitation by ureolytic subsurface bacteria." *Geomicrobiol. J.*, 17(4), 305–318.
Gat, D., Ronen, Z., and Tsesarsky, M. (2016). "Soil bacteria population dynamics following stimulation for ureolytic microbial-induced $CaCO_3$ precipitation." *Environ. Sci. Technol.*, 50(2), 616–624.
Gat, D., Tsesarsky, M., Wahanon, A., and Ronen, Z. (2014). "Ureolysis and MICP with model and native bacteria: Implications for treatment strategies." *Geo-Congress 2014 Technical Papers*, ASCE, Reston, VA, 1713–1720.
Gibson, S., and Sewell, G. (1992). "Stimulation of reductive dechlorination of tetrachloroethene in anaerobic aquifer microcosms by addition of short-chain organic acids or alcohols." *Appl. Environ. Microbiol.*, 58(4), 1392–1393.
Gomez, M. G., et al. (2015). "Field-scale bio-cementation tests to improve sands." *Ground Improv.*, 168(3), 206–216.
Gomez, M. G., Anderson, C. M., DeJong, J. T., Nelson, D. C., and Lau, X. (2014). "Stimulating in situ soil bacteria for bio-cementation of sands." *Geo-Congress 2014 Technical Papers*, ASCE, Reston, VA, 1674–1682.
Gomez, M. G., Anderson, C. M., Graddy, C. M. R., DeJong, J. T., Nelson, D. C., and Ginn, T. R. (2016). "Large-scale comparison of bioaugmentation and biostimulation approaches for biocementation of sands." *J. Geotech. Geoenviron. Eng.*, 10.1061/(ASCE)GT.1943-5606.0001640, 04016124.
Hammes, F., Boon, N., de Villiers, J., Verstraete, W., and Siciliano, S. D. (2003). "Strain-specific ureolytic microbial calcium carbonate precipitation." *Appl. Environ. Microbiol.*, 69(8), 4901–4909.
Hobbie, J. E., Daley, R. J., and Jasper, S. (1977). "Use of nucleopore filters for counting bacteria by fluorescence microscopy." *Appl. Environ. Microbiol.*, 33(5), 1225–1228.
ImageJ [Computer software]. National Institutes of Health, Bethesda, MD.
Knorst, M. T., Neubert, R., and Wohlrab, W. (1997). "Analytical methods for measuring urea in pharmaceutical formulations." *J. Pharm. Biomed. Anal.*, 15(11), 1627–1632.
Lauchnor, E. G., Topp, D. M., Parker, A. E., and Gerlach, R. (2015). "Whole cell kinetics of ureolysis by *Sporosarcina pasteurii*." *Eur. J. Appl. Microbiol.*, 118(6), 1321–1332.
Litchman, E. (2010). "Invisible invaders: Non-pathogenic invasive microbes in aquatic and terrestrial ecosystems." *Ecol. Lett.*, 13(12), 1560–1572.
Martinez, B., et al. (2013). "Experimental optimization of microbial induced carbonate precipitation." *J. Geotech. Geoenviron. Eng.*, 10.1061/(ASCE)GT.1943-5606.0000787, 587–598.
Martinez, B. C., and DeJong, J. T. (2009). "Bio-mediated soil improvement: Load transfer mechanisms at the micro- and macro-scales." *Advances in ground improvement*, ASCE, Reston, VA, 242–251.
Mobley, H. L., Island, M. D., and Hausinger, R. P. (1995). "Molecular biology of microbial ureases." *Microbiol. Rev.*, 59(3), 451–480.
Montoya, B. M., et al. (2012). "Fabrication, operation, and health monitoring of bender elements for aggressive environments." *Geotech. Test. J.*, 35(5), 728–742.
Montoya, B. M., and DeJong, J. (2015). "Stress-strain behavior of sands cemented by microbially induced calcite precipitation." *J. Geotech. Geoenviron. Eng.*, 10.1061/(ASCE)GT.1943-5606.0001302, 04015019.
Montoya, B. M., DeJong, J., and Boulanger, R. (2013). "Dynamic response of liquefiable sand improved by microbial-induced calcite precipitation." *Géotechnique*, 63(4), 302–312.
PHREEQC version 3 [Computer software]. U.S. Geological Survey, Reston, VA.
Pritchard, P., and Costa, C. (1991). "EPA's Alaska oil spill bioremediation project." *Environ. Sci. Technol.*, 25(3), 372–379.
Pritchard, P., Mueller, J., Rogers, J., Kremer, F., and Glaser, J. (1992). "Oil spill bioremediation: Experiences, lessons, and results from the Exxon Valdez oil spill in Alaska." *Biodegradation*, 3(2), 315–335.
Schneider, C. A., Rasband, W. S., and Eliceiri, K. W. (2012). "NIH Image to ImageJ: 25 years of image analysis." *Nat. Methods*, 9(7), 671–675.
Stocks-Fisher, S., Galinat, J. K., and Bang, S. S. (1999). "Microbiological precipitation of $CaCO_3$." *Soil Biol. Biochem.*, 31(11), 1563–1571.
Tobler, D., et al. (2011). "Comparison of rates of ureolysis between *Sporosarcina pasteurii* and an indigenous groundwater community under conditions required to precipitate large volumes of calcite." *Geochim. Cosmochim. Acta*, 75(11), 3290–3301.
Truex, M. J., et al. (2009). "Hanford 100-D area biostimulation treatability test results." *PNNL-18784*, Pacific Northwest National Laboratory, Richland, WA.
van Paassen, L. A. (2011). "Bio-mediated ground improvement: From laboratory experiment to pilot applications." *Geo-Frontiers 2011*, ASCE, Reston, VA, 4099–4108.
Whiffin, V., van Paassen, L., and Harkes, M. (2007). "Microbial carbonate precipitation as a soil improvement technique." *Geomicrobiol. J.*, 24(5), 417–423.